

Cause of Plasmasphere Corotation Lag

J. L. Burch¹, J. Goldstein¹, and B. R. Sandel²

¹Southwest Research Institute

²University of Arizona

It is hypothesized that the recently observed plasmasphere corotation lag is caused by a corresponding corotation lag in the upper ionosphere. Rotation rates of long-lived plasmaspheric notches are compared to ionospheric drifts observed on DMSP spacecraft in the same longitude sectors. Good agreement between the two observations is found, and the cause of the corotation lag is identified as the ionospheric disturbance dynamo. The observed corotation lag will have to be accounted for in future magnetospheric convection models, which until now have assumed strict plasmasphere corotation.

Introduction

Sandel et al. [2003] used localized low-density regions (or notches) as markers to track the rotation of the plasmasphere. Such notches have been observed to persist for periods as long as 60 hours, during which time they can be tracked for up to six hours of each 14-hour IMAGE [*Burch*, 2000] orbit when the spacecraft is hovering near apogee. Sandel et al. found that the plasmasphere rotation rate at $L \sim 2-3$ lags corotation by up to 10-15%. Although no cause of the corotation lag was given, its observation has strong implications for magnetospheric convection models [e. g., *Grebowsky*, 1970; *Spiro et al.*, 1981; *McIlwain*, 1986; *Weiss et al.*, 1997], which have for many years assumed a corotation electric field inside a “shielding distance” at which the Region-2 field-aligned current system shields the inner magnetosphere from the electric fields produced by the interaction of the magnetosphere with the solar wind. It is worth noting that the corotation lag observed by *Sandel et al.* [2003] is not caused by the simple penetration of outer magnetospheric electric fields into the plasmasphere, although such effects surely occur, because it does not show a strong local-time dependence. Penetration fields would produce a generally sunward flow that at these L values, which would cause a higher rotation rate in the dawn hemisphere and a lower rate in the dusk hemisphere.

As noted by *Hill* [1979], planetary plasma corotation is generally not expected to break

down until the point at which the corotation velocity exceeds the Alfvén speed, although mass loading by plasma flowing outward from the planetary ionosphere can move this point much closer to the planet. Estimates of the breakdown distance for both Jupiter and the Earth are coincidentally ~ 60 planetary radii [Hill, 1979]. In a localized sense in the Jovian magnetosphere, a variable corotation lag averaging about 5% has been observed for the Io plasma torus (at 6 Jovian radii) [Brown, 1994]. Pontius and Hill [1982] have shown that for this level of corotation lag local plasma production within the Io torus would be required, and Brown [1994] has estimated an ion production rate between 2000 and 3000 kg sec⁻¹, which results from the large volcanic and atmospheric gas source at Io. The IMAGE observations, which show a percentage corotation lag at 2-3 Earth radii two to three times that in the Io plasma torus (even though there is no local gas source as there is at Io), suggests a strong influence but one that is not related to mass loading. The simplest conclusion, and the hypothesis upon which this study was based, is that a departure from corotation of the midlatitude ionosphere is the direct cause of plasmasphere subcorotation. Ionospheric corotation is generally assumed to hold in plasmaspheric convection models; however, radar and satellite observations [e.g., Wand, 1983; Heelis and Coley, 1992] have for many years shown that a significant departure from corotation, especially at midlatitudes, does routinely occur. Furthermore, its cause has been suggested to be the ionospheric disturbance dynamo [Blanc and Richmond, 1980]. In addition to an ionospheric corotation lag, the upper atmosphere and ionosphere at times exhibit superrotation [Rishbeth, 1972]. Whether corotation, subcorotation, or superrotation occurs at any given place and time depends upon the confluence of numerous effects including, but not limited to, angular momentum conservation, solar tidal forces, auroral heating, and ionospheric currents.

Two data sources are used in this study—EUV images of the plasmasphere from the IMAGE satellite and ion drift measurements from the DMSP F12, F13 and F15 satellites. These data, applied to one of the events published by Sandel *et al.* [2003], demonstrate that subcorotation of the ionosphere can explain fully the observed subcorotation of the plasmasphere. The implications of this result are important for the development of accurate models of magnetospheric convection electric fields, which must include either real-time empirical data or accurate models of global ionospheric drifts if accurate descriptions of inner magnetosphere convection are to be obtained. For example, a 10-15% corotation lag will cause the boundary between open and closed convection paths to move significantly closer to the Earth

than would be predicted by a model involving strict plasmaspheric corotation.

Observations

Figure 1 shows a sequence of plasmasphere images obtained on April 6-8, 2001 by the EUV instrument [Sandel *et al.*, 2000] on the IMAGE satellite. In each panel is an EUV image that has been mapped to the magnetic equator in L and magnetic local time (MLT). (see Roelof and Skinner [2000]; Goldstein *et al.* [2003b]; Dent *et al.* [2003]). For the line of sight corresponding to the center of each pixel, the mapping procedure identifies the dipole field line of minimum L value touched by the line of sight and assigns the brightness of the pixel to the [L, MLT] coordinates of that field line. This procedure is based on the fact that the plasmaspheric density falls off rapidly with L ($\sim L^{-4}$) and is most accurate where sharp edges occur in the density profile (e. g., at the plasmopause). The color scale intensity is proportional to the log of the line-of-sight integrated He⁺ column abundance. In the center of each image, which is a view from above the north pole, the apparent size and location of the Earth are indicated by the black and white circle. The Sun is to the right in each panel, and a faint shadow extends antisunward from the Earth on the nightside. The plasmasphere is the greenish-to-white haze of 30.4-nm light that surrounds the Earth; close to the Earth the emissions are dominated by airglow from neutral helium and O⁺.

In each panel of Figure 1 a red line is drawn radially outward from the Earth, and in the first panel the line bisects a plasmaspheric density notch. In subsequent panels the red line moves with the rotation of the Earth, while the notch, which is marked with a yellow arrow, is clearly seen to lag significantly behind corotation over the 55-hour period covered by the five panels.

In order to test the hypothesis that the corotation lag of plasmaspheric notch features follows the overall plasmasphere and ionosphere rotation rate, drift-meter data from the DMSP spacecraft F12, F13 and F15 were compiled for the magnetic longitude sector 100° - 180°. This range of longitudes bounds the location of the notch throughout its period of observation beginning on April 6, 2001. These data are plotted in Figure 2 with the six-hour MLT sectors color coded. Also shown in each panel are the Kp values during the respective ten-hour periods. Positive values of the ordinate correspond to eastward drift, which is defined relative to the 96° orbital plane of DMSP so that only drift meter data, and not RPA data are used. The rationale for this restriction is the same as that used by Heelis and Coley [1992]. The drift meter data are obtained with higher time resolution, are affected to a lesser degree than the RPA data by sources

of error such as spacecraft potential variations, and for the midlatitude region occupied by the outer plasmasphere are very close to representing geographic or magnetic east-west flow velocities.

Each panel in Figure 2 covers a ten-hour time period beginning with the first observation of the plasmaspheric notch early on April 6, 2001. In each panel, high and variable values of east-west drift associated with the auroral oval are clearly seen at latitudes above $50^\circ - 60^\circ$. At low and midlatitudes, the drifts are generally within 100 m/s of the corotation velocity, which is denoted by the 0-line in Figure 2; but since the corotation velocity at the DMSP altitude of ~ 850 km and at 45° magnetic latitude is only ~ 325 m/s, the variations are quite significant. As shown by the color-coded MLT sectors, there are significant dependencies on MLT and latitude, and these features of the data in Figure 2 are consistent with those published by *Heelis and Coley* [1992]. For example, a supercorotation at midnight for magnetic latitudes near 25° and a subcorotation at all MLTs remote from noon at midlatitudes are clearly seen in Figure 2 as well as in Figure 3 of *Heelis and Coley* [1992].

In Figure 3, the observed location of the plasmaspheric density notch in UT-MLT is plotted by the red data points. The position of a corotating feature, beginning at the first observation of the notch at 03:03 UT on April 6, 2001, is shown by the blue line. Finally, the predicted locations of the notch after each of the first five ten-hour periods of notch observation (the first five panels of Figure 2) are shown by the green data points, which are derived from the average east-west drift velocity at latitudes between 40° and 45° . This latitude range represents that of the Earthward edge of the notch. Extension of the drift data averages to higher latitudes yields comparable results but with larger errors because of contamination by auroral drifts.

Discussion and Conclusions

The data shown in Figures 1-3 show clearly that the outer plasmasphere, as traced by a density notch feature, rotates at a rate significantly slower (10-15%) than corotation, as first noted by *Sandel et al.* [2003]. Analysis of DMSP data for the same spatial and temporal locations occupied by the notch show that the departures from corotation observed in the midlatitude upper ionosphere are fully capable of predicting the plasmaspheric corotation lag when the MHD approximation is assumed to hold for the region above 850 km altitude. Thus, while the observed corotation lag should not be surprising, it is considerably at odds with the usual assumption of

strict corotation that has been used in all magnetospheric convection models that have been in use for at least the past three decades.

The cause of the corotation lag at midlatitudes is most likely the ionospheric disturbance dynamo as described by *Blanc and Richmond* [1980]. In its simplest terms, this phenomenon involves the input of energy to the auroral ionosphere by particle precipitation and joule heating. This heat input produces equatorward winds that carry gas into the midlatitude region where the rotational velocity of the Earth is increasing. Conservation of angular momentum within this gas (or equivalently the Coriolis force), which originated at higher latitudes, causes it to lag behind the Earth's rotation. This lag at latitudes just below the auroral oval is clearly seen in the DMSP data of Figure 2.

The most obvious result of a slower plasmasphere rotation rate in magnetospheric convection models is that the boundary between open and closed convection paths will move closer to the Earth. In addition, the details of the convection patterns throughout the inner magnetosphere will be affected since at every point the corotation electric field and any externally imposed electric fields are added to produce a total electric field.

One can estimate the effects of the corotation lag by considering the analytical Volland-Stern electric potential model ($\Phi = V_C/R + V_M R^2 \sin(\theta)$) [Volland, 1973; Stern, 1975] where V_C and V_M are the corotation potential and the magnetospheric convection potential, respectively, and θ is an azimuthal angle measured counterclockwise from midnight. The location of the last closed equipotential (LCE) in the equatorial dusk meridian ($\theta = 270^\circ$, $R=L$) can be obtained by setting E (the sum of the corotation electric field, E_C , and the magnetospheric electric field, E_M) equal to zero, i. e.,

$$E_R = -\partial\Phi/\partial L = -V_C L^{-2} + 2V_M L = 0, \text{ or}$$

$$L^3 = V_C/(2V_M).$$

Thus the L-value of the LCE dusk crossing in the equatorial plane varies as the cube root of the corotation potential, or, for a 15% subcorotation, as $(0.85)^{1/3}$. *Maynard and Chen* [1975] have derived a specific Kp dependence of V_M , which can be used to show, for example, that for Kp=4 the equatorial dusk meridian LCE will lie at $L = 5.16$ for strict corotation but at $L = 4.89$ for a 15% corotation lag.

Since the observed, and now predicted, corotation lag is significant (10-15%), it is important that future convection electric-field models treat this phenomenon accurately either by

incorporating empirical ionospheric data or by including a realistic model of midlatitude ionospheric convection that reflects the systematic variations with latitude and local time (as illustrated in Figure 2 and previously presented by *Heelis and Coley*, [1992]) that are known to occur.

Acknowledgements

This research was supported by NASA Contract No. NAS5-96020 with Southwest Research Institute. A helpful discussion with Dr. Don Carpenter is gratefully acknowledged. Cynthia Farmer provided significant assistance with data reduction. The DMSP drift-meter data were provided by the PI, Dr. R. A. Heelis, through the UT-Dallas DMSP web site.

References

- Blanc, M., and A. D. Richmond, The ionospheric disturbance dynamo, *J. Geophys. Res.*, **85**, 1669-1686, 1980.
- Brown, M. E., Observation of mass loading in the Io plasma torus, *Geophys. Res. Lett.*, **21**, 847-850, 1994.
- Burch, J. L., IMAGE mission overview, *Space Sci. Rev.*, **91**, 1-14, 2000.
- Dent, Z. C., I. R. Mann, F. W. Menk, J. Goldstein, C. R. Wilford, M. A. Clilverd, and L. G. Ozeke, A coordinated ground-based and IMAGE satellite study of quiet-time plasmaspheric density profiles, *Geophys. Res. Lett.*, **30**(12), 1600, doi:10.1029/2003GL016946, 2003.
- Goldstein, J., M. Spasojevic, P. H. Reiff, B. R. Sandel, W. T. Forrester, D. L. Gallagher, and B. W. Reinisch, Identifying the plasmopause in IMAGE EUV data using IMAGE RPI in situ steep density gradients, *J. Geophys. Res.*, **108**(A4), 1147, doi:10.1029/2002JA009475, 2003.
- Grebowsky, J. M., Model study of plasmopause motion, *J. Geophys. Res.*, **75**, 4329, 1970.
- Heelis, R. A., and R. J. Coley, East-west ion drifts at mid-latitudes observed by Dynamics Explorer 2, *J. Geophys. Res.*, **97**, 19,461-19,469, 1992.
- Hill, T. W., Inertial limit on corotation, *J. Geophys. Res.*, **84**, 6554-6558, 1979.
- Maynard, N. C., and A. J. Chen, Isolated cold plasma regions: Observations and their relation to possible production mechanisms, *J. Geophys. Res.*, **80**, 1009-1013, 1975.
- McIlwain, C.E., A Kp dependent equatorial electric field model, *Adv. Space Res.*, **6**, 187, 1986.
- Pontius, D. H., and T. W. Hill, Departure from corotation of the Io plasma torus: local plasma production, *Geophys. Res. Lett.*, **9**, 1321-1324, 1982.
- Rishbeth, H., Superrotation of the upper atmosphere, *Rev. Geophys. Space Phys.*, **10**, 799-819, 1972.

- Roelof, E. C. and A.J. Skinner, Extraction of ion distributions from magnetospheric ENA and EUV images, *Space Science Reviews*, 91, 437-459, 2000.
- Sandel, B. R., et al., The Extreme Ultraviolet (EUV) imager investigation for the IMAGE mission, *Space Sci. Rev.*, 2000.
- Sandel, B. R., J. Goldstein, D. L. Gallagher, and M. Spasojevic, EUV Observations of the Structure and Dynamics of the Plasmasphere, *Space Sci. Rev.*, in press, 2003.
- Spiro, R. W., M. Harel, R. A. Wolf, and P. H. Reiff, Quantitative simulation of a magnetospheric substorm, 3, Plasmaspheric electric fields and evolution of the plasmopause, *J. Geophys. Res.*, 86, 2261, 1981.
- Stern, D. P., The motion of a proton in the equatorial magnetosphere, *J. Geophys. Res.*, 80, 595-599, 1975.
- Volland, H., A semiempirical model of large-scale magnetospheric electric fields, *J. Geophys. Res.*, 78, 171-180, 1973.
- Wand, R. H., Seasonal variations of lower thermospheric winds from the Millstone Hill incoherent scatter radar, *J. Geophys. Res.*, 93, 699-708, 1988.
- Weiss, L. A., R. L. Lambour, R. C. Elphic, and M. F. Thomsen, Study of plasmaspheric evolution using geosynchronous observations and global modeling, *Geophys. Res. Lett.*, 24, 599, 1997.

Figure Captions

Figure 1. EUV images in 30.4-nm light plotted in L-MLT on April 6-8, 2001. Each frame of EUV data is an accumulation of 30.4-nm light from five two-minute spin periods of the IMAGE satellite. Each observed pixel of column-integrated EUV irradiance is mapped to the equator along the dipole field line corresponding to the minimum-L intersection of its field of view [Goldstein *et al.*, 2003]. The red radial line, which bisects a plasmaspheric density notch in the first panel, tracks the Earth's rotation in the subsequent panels in which the notch is noted with a yellow arrow.

Figure 2. Drift-meter data from the DMSP 12, 13 and 15 satellites for six ten-hour periods during the observation of the plasmaspheric notch shown in Figure 1. Each plot is a composite of data from all three satellites whenever they were between geomagnetic longitudes of 100° and 180° , which defines the longitude sector containing the notch throughout its period of observation. Noon (09-15 UT), midnight (21-03 UT), dawn (03-09 UT) and dusk (15-21 UT) data are color coded. Kp values for the ten-hour period are listed at the top of each plot.

Figure 3. Plot in MLT and UT of position of the plasmaspheric notch from its first observation at 03:05 UT on April 6, 2001 until 12:03 UT on April 8, 2001 (red data points); the locations predicted by corotation (blue line), and the locations predicted by the DMSP data in Figure 2 within the geomagnetic latitude interval 40° - 45° (green data points).

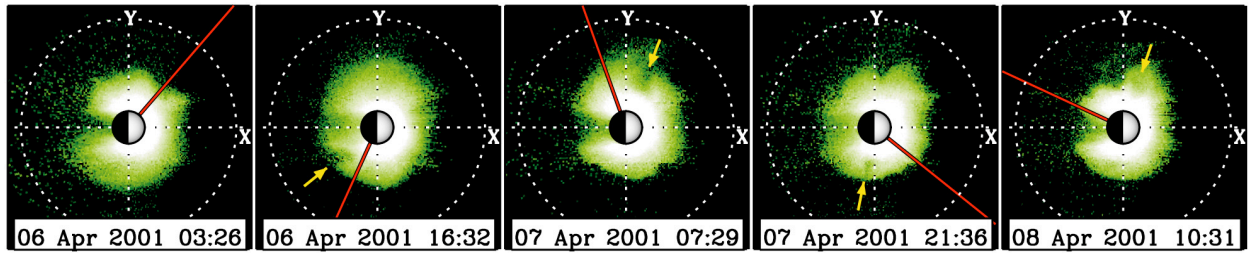


Figure 1

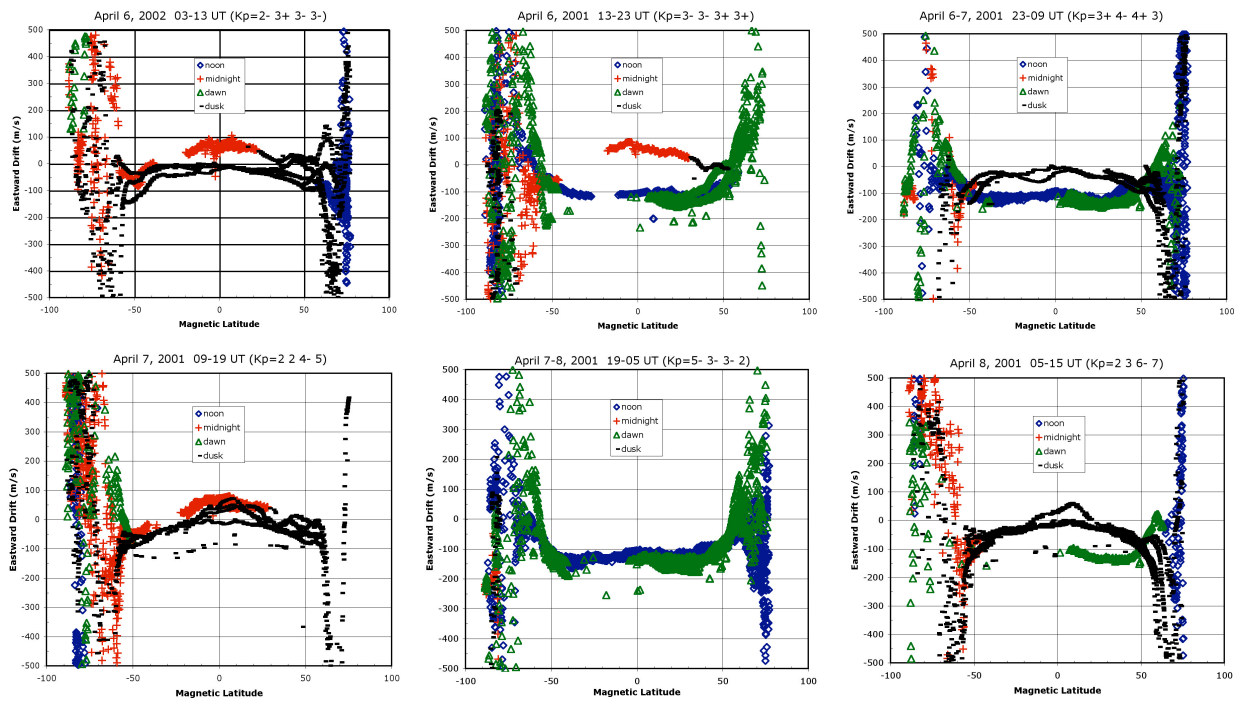


Figure 2

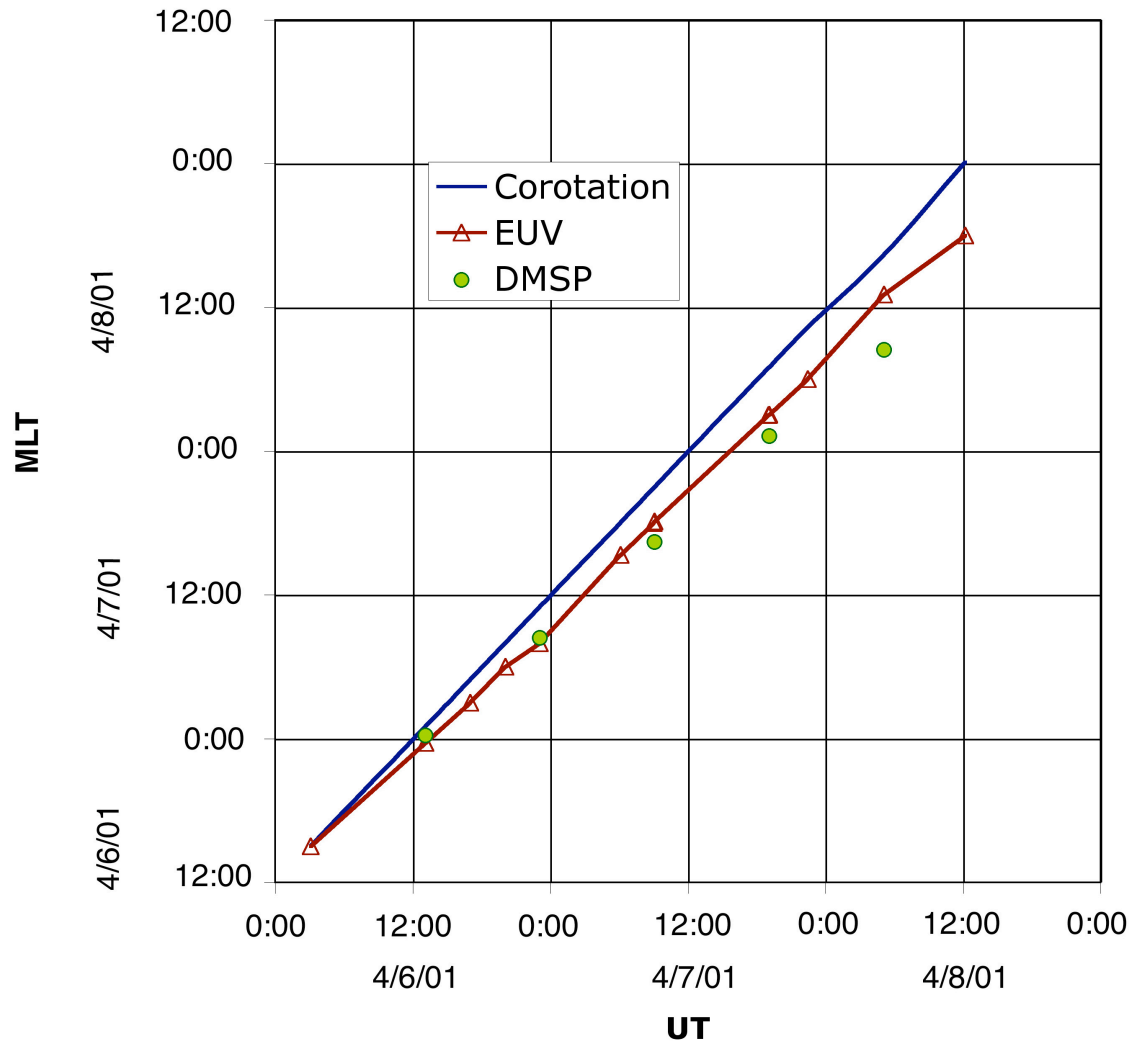


Figure 3